ELSEVIER

Physica B 248 (1998) 14–24

PHYSICA B

Surface and interfacial magnetic diffuse scattering

Masayasu Takeda[a,*], Yasuo Endoh[a], Atsushi Kamijo[b], Jun'ichiro Mizuki[c]

[a] *Physics Department, Graduate School of Science, Tohoku University, Aramaki Aobaku, Sendai 980-77, Japan*
[b] *Fundamental Research Laboratories, NEC Corporation, 1-1-4 Miyazaki, Kawasaki 216, Japan*
[c] *SPring-8, Japan Atomic Energy Research Institute, SPring-8, Kamigori-cho, Ako-gun, Hyogo 678-12, Japan*

Abstract

We investigated surface and interfacial roughness in the magnetic multilayers by using neutron off-specular diffuse scattering. Single crystals of Fe/Cr multilayers with different interfacial roughnesses between Fe and Cr layers were used as samples. Interfacial roughness appeared around the antiferromagnetic Bragg peak from the antiferromagnetic structure in the profile of the off-specular diffuse scattering. The profile was very sensitive to the interfacial roughness which were modified by substrates, condition of crystal growth and external magnetic fields. This indicates that neutron off-specular diffuse scattering is a promising tools for the investigation of interfacial magnetism.

Keywords: Neutron off-specular diffuse scattering; Surface; Interface; Roughness; Magnetic disorder

1. Introduction

X-ray off-specular diffuse scattering measurements have been widely used for the investigation of surface and interfacial roughness in various multilayers. In the magnetic multilayers, the interfacial roughness originating from in atomic disorders is expected to cause magnetic disorders at the surface or interfaces as well as the enhancement or reduction of magnetic moments. Because of very small cross section available to magnetic moments, X-rays have not been used for the study of magnetism especially in the surface and interfacial magnetism. Recently it is shown that the resonant X-ray scattering enables the detection of surface magnetism, and it is going to the extended to interfacial magnetism hopefully [1].

Interaction between neutron and magnetic moments is much larger than with X-rays, and neutron shows the optical phenomena as well as X-ray and visible light. Therefore, neutron is potentially an excellent probe of surface and interfacial magnetism by using the same technique as X-ray. However, neutron has not been used for such an investigation. This is mainly because the luminosity of a neutron source is much less than that of X-ray, synchrotron sources. The less intensity makes it difficult to perform experiments with well-collimated beams which are essential to observe fine structures appearing in the profile of off-specular

* Corresponding author. Fax: + 81 22 217 6489; e-mail: takeda@iiyo.phys.tohoku.ac.jp.

0921-4526/98/$19.00
PII: S0921-4526(98)00196-3

diffuse scattering like the Yoneda peak [2]. On the other hand, neutron has much less absorption cross sections to most of the materials than X-ray. We found out that the transparency gave new aspects of the off-specular diffuse scattering. In this paper we report the neutron off-specular diffuse scattering measurements of Fe/Cr multilayers with various interfacial roughnesses which clearly appears in the different profiles of off-specular diffuse scattering around the Bragg peaks from antiferromagnetic Fe/Cr bilayers.

The Fe/Cr multilayer is one of the magnetic multilayers which shows a giant magnetoresistance (GMR) effect [3]. The GMR effect is the phenomenon that negative resistivity change whose magnitude is very large compared with the conventional bulk magnets is induced by external magnetic fields. The GMR effect is observed in the magnetic multilayers which consists of alternative magnetic and nonmagnetic layers. In the multilayer ferromagnetic moments in the magnetic layers are coupled antiferromagnetically through adjacent nonmagnetic layers. This antiferromagnetic exchange coupling oscillates with the nonmagnetic layer thickness with a period ranging from 12 to 21 Å [4]. The GMR effect only appears in the multilayers with the antiferromagnetic coupling. It is experimentally concluded that the resistivity strongly depends on the alignment of the adjacent ferromagnetic layer. Since such spin-dependent scattering of conduction electrons cannot be expected to occur in the bulk or at the perfect flat interface between magnetic and nonmagnetic layers, the interfacial roughness, the atomic mixing at the interfaces, has now been considered to be essential to the GMR effect.

2. Experimental

2.1. Samples

Single crystals of Fe/Cr multilayers are prepared by molecular beam epitaxy at NEC Corp. [5,6]. A [Fe (3 nm)/Cr (1 nm)] bilayer is grown $N(N = 30, 51, 80)$ times on the seed Cr layer under which Nb buffer layer is grown on Al_2O_3 $(1\,\bar{1}\,0\,2)$ or MgO $(1\,0\,0)$ substrates. The shape of the sample is rectangular whose dimensions are typically $30 \times 40\ mm^2$, the crystal face being the $(1\,0\,0)$ plane of bcc-Fe and bcc-Cr atoms. The thickness of Fe and Cr layers in the Fe/Cr bilayer is designed to obtain the largest GMR effect. The samples are named as 1 ($N = 80$ on sapphire), 2 ($N = 51$ on MgO), 3 ($N = 30$ on sapphire) and 4 ($N = 30$ on MgO).

2.2. Reflection measurements of the TOP spectrometer

Neutron reflection measurements were performed on the TOP spectrometer installed at the pulsed neutron source (KENS) at National Laboratory for High Energy Physics. TOP is a pulsed-polarized neutron time of flight spectrometer with optical polarizer which utilizes wavelength band of 3–18 Å from a solid methane cryogenic moderator. The band was separated into two sub bands, 3–9 Å and 11–18 Å by a band selector of disk chopper in order to avoid frame-overlap of neutrons. Fig. 1a shows the schematic representation of experimental setup for reflection measurements on the TOP spectrometer. Unpolarized neutrons were introduced to neutron polarizers, and outgoing polarized neutrons are collimated by a pair of horizontal slits, s_1 and s_2, before the sample. The vertical collimation of neutrons are fixed by a pair of vertical slits of 20 mm height. The one-dimensional position-sensitive detectors (PSD) were used as a detecting system. An effective length of the PSD is 640 mm long which can be divided up to 256 positional channels. The PSD are horizontally arranged in three lines in order to detect neutrons of 20 mm height. At each positional channel neutrons are counted according to time of flight from moderator to the PSD during 50 ms at each pulse. The time channel can be divided into up to 4096 channels. The number of positional channels was set to be 64 and that of the time channel 32 in these experiments. Fig. 1b graphically explained the way of reflection measurements using pulsed neutrons and the PSD detecting system. The sample plane is aligned vertically, and the scattering vector, $\boldsymbol{Q}$, is in the horizontal plane. Incident neutrons hit the sample with incident angle of θ_1. A part of the

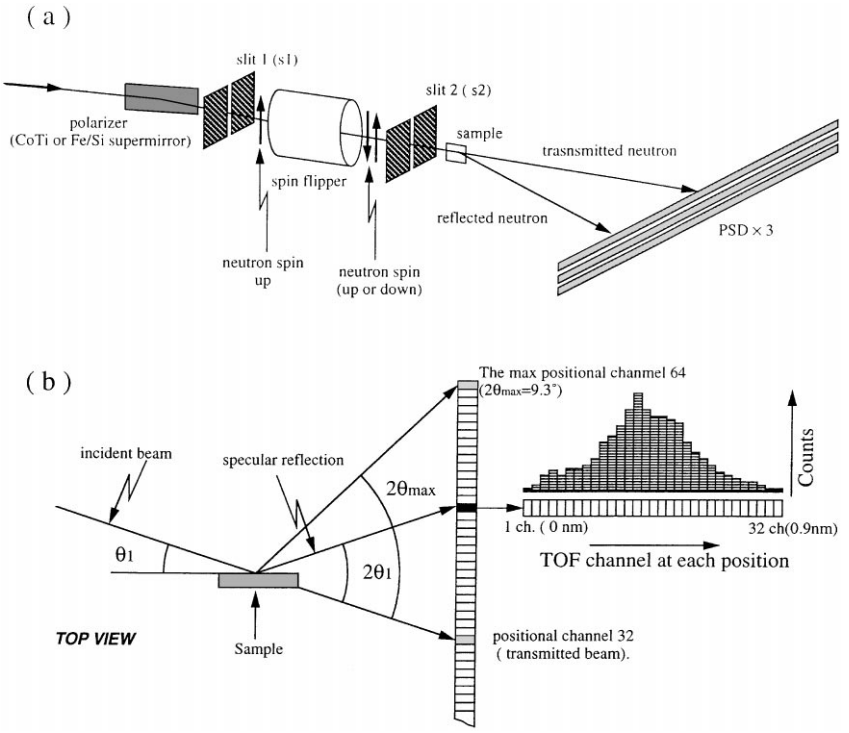

Fig. 1. Schematic representation of (a) the pulsed cold polarized neutron spectrometer TOP and (b) reflectivity measurement using position sensitive detector and TOF method.

neutron is reflected with the reflection angle of $2\theta_1$ in the case of specular reflection and hits the corresponding positional channel in the vicinity of which intensities of off-specular diffuse scattering are observed. The rest of neutrons goes through the sample and are detected at the center position of the PSD.

2.3. *Specular and off-specular diffuse scattering measurements on the TOPAN spectrometer*

Measurements of detailed profile of off-specular diffuse scattering have been done on a conventional triple-axis spectrometer, TOPAN, installed at JRR-3M in Tokai Establishment, Japanese Atomic Energy Research Institute (JAERI) (Fig. 2). The incident wavelength was fixed at 0.24 nm by a PG(002) monochrometer, and the higher-order reflections were removed by a PG filter before the sample. The analyzer, PG(002), was used only to reduce background from the incident beams. The beam collimation is defined by four Soller collimators as shown in Fig. 2. The sample was set in such a way that the scattering vector, $\boldsymbol{Q}$, is normal to the sample plane in the θ–2θ measurements. Hereafter, the direction normal to the sample plane is defined as the z-axis and the sample plane as the xy-plane. Therefore, the θ–2θ scan corresponds to the Q_z scan in the reciprocal space. The measurements of off-specular diffuse scattering were done by the transverse scan (Q_r scans for the constant Q_z) as shown in the inset of Fig. 2. The transverse scan is similar to the rocking scan of the fixed scattering angle in the small Q_r region. Here we assume that there is no anisotropy in the sample plane and define Q_r which indicates the component in the xy-plane of the scattering vector, i.e. $|Q_r| \equiv \sqrt{Q_x^2 + Q_y^2}$. External magnetic fields were applied up to 1 T in the sample plane by an electromagnet.

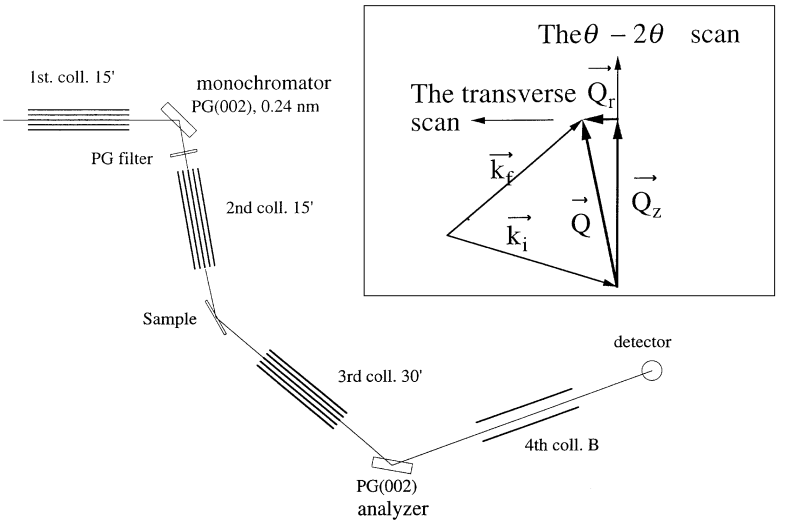

Fig. 2. Experimental setup of the TOPAN spectrometer in JRR-3M for off-specular diffuse scattering measurement. Inset shows the difference between the ordinary longitudinal scan and the transverse one.

3. Results

3.1. Reflectivities measured on the TOP spectrometer

Fig. 3 is the specular reflectivity curves of sample 1 measured by the TOP spectrometer in the absence of magnetic fields at room temperature. In order to cover the wide Q range, both subbands of neutrons were used in the fixed incident angle of 1.1 and 2.7°. The curve was obtained only using the data at the positional channel 51 which was satisfied with specular condition. Total reflection occurs at 0.018 $Å^{-1}$. Antiferromagnetic Bragg peak from the antiferromagnetic structure of Fe/Cr bilayer with twice the lattice spacing of the bilayer of 4 nm appears at 0.07 $Å^{-1}$ and the Bragg peak from the Fe/Cr bilayer itself at 0.13 $Å^{-1}$. Hereafter, we name the former the $\frac{1}{2}$ peak and the latter the first peak. Fig. 4a and b show the positional channel dependence of intensities obtained in the measurements by integration over the TOF channels corresponding to 3–9 Å and 11–18 Å, respectively. The peak at channels 32 and 33 in the spectrum are due to the direct beam, which did not pass through the sample and transmitted neutrons which underwent small refraction. The reflected beam under the specular condition was detected at positional channel 51, however, this main peak has an additional small peak at channel 45. The additional peak and the other intense peak at channel 57 were also visible in Fig. 4b. As shown in Fig. 5 contour map of intensities of reflected neutrons in which the horizontal axis is the number of position channel of the PSD (scattering angle) and the vertical axis is the number of time channel (wavelength of neutrons)

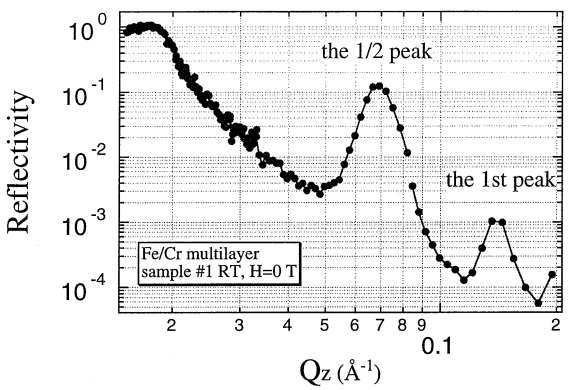

Fig. 3. Specular reflectivity of Fe/Cr multilayer sample 1 in the absence of magnetic fields measured on TOP.

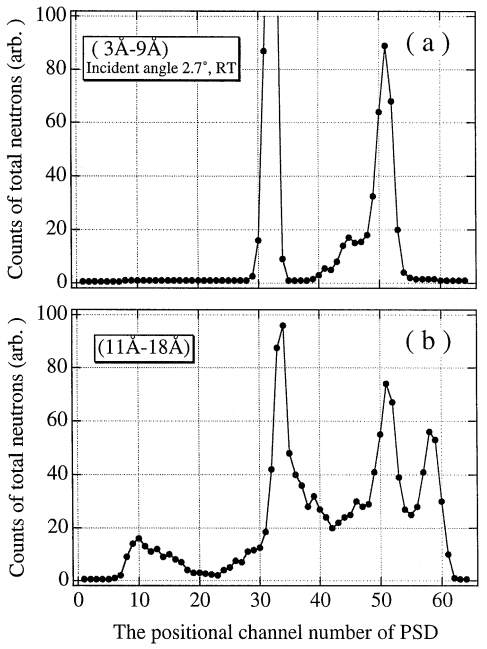

Fig. 4. The positional channel dependence of integrated intensities of neutron over TOF channel. The positional channel corresponds to the scattering angle.

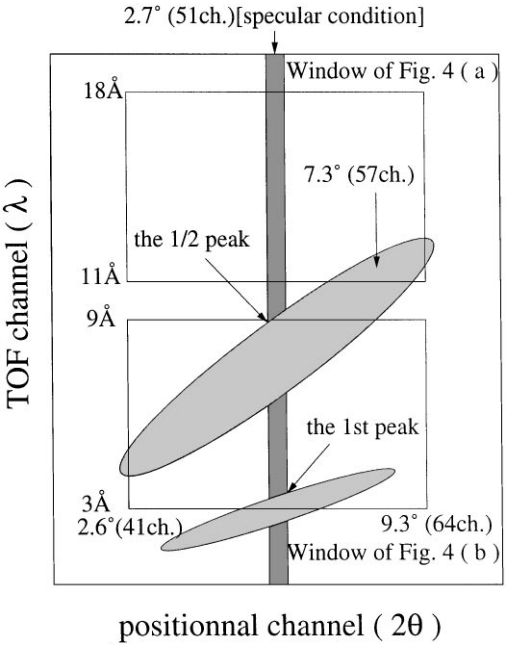

Fig. 6. Schematic representation of the wavelength – scattering angle window for the experiments in Fig. 5.

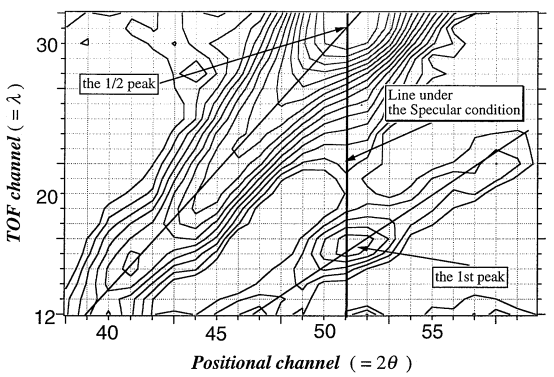

Fig. 5. Contour map of reflected intensities of sample 1. The horizontal axis is related to the scattering angle and the vertical one to the wavelength of neutrons. Two broad Bragg peaks are observed centered at (51, 16) and (51, 31) points.

helps to explain the origin of these extra peaks. The data on the vertical straight line, $P_{ch} = 51$ ($2\theta = 2.7^{\circ}$), correspond to the specular reflectivities. The peak at (51, 16) is the $\frac{1}{2}$ peak and that at (51, 2) is the first peak. The map shows that the peaks, especially the $\frac{1}{2}$ peak, are widely spread along the line of constant Q_z. The angle-wavelength window of Fig. 4a and b are schematically displayed in Fig. 6. It is obvious that the extra reflection at channel 57 is the foot of diffuse scattering around the $\frac{1}{2}$ peak. Such large magnetic diffuse scattering suggests that there exists an in-plane magnetic disorder at the interfaces between the Fe layers and the Cr layers.

3.2. The profile of off-specular diffuse scattering

The θ–2θ scan, Q_z scan, of sample 1 is displayed in Fig. 7a, and the profile of off-specular diffuse scattering around the $\frac{1}{2}$ and the first peaks are shown in Fig. 7b and c as a function of Q_r, respectively. These data were taken in the absence of external magnetic fields. The profile of the Q_r scan seems to be composed of sharp specular central component and additional broad off-specular diffuse scattering. Intense off-specular diffuse scattering is clearly observed at the $\frac{1}{2}$ peak. On the other

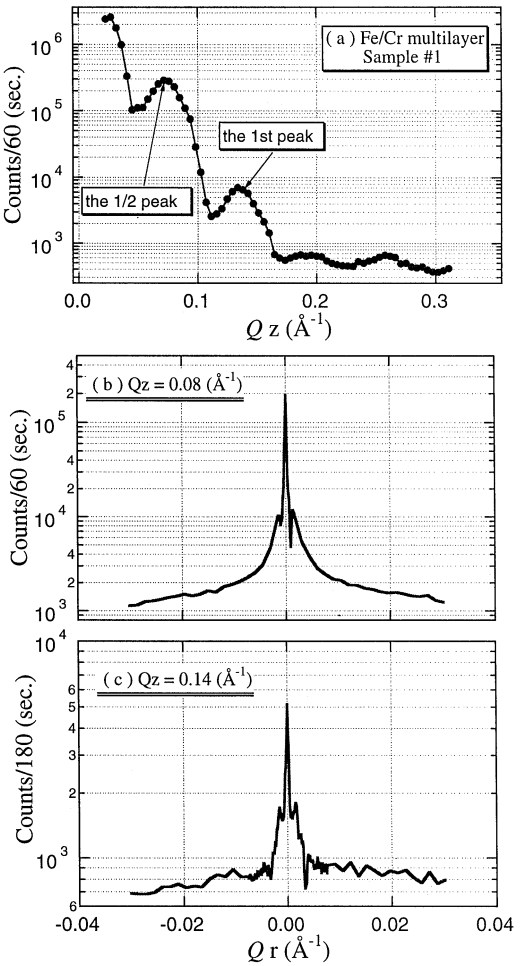

Fig. 7. The Q_z (a) and the Q_r dependencies of reflected intensities of neutrons in sample 1 around the antiferromagnetic Bragg peak (b) and the Bragg peak of Fe/Cr bilayer (c).

hand, around the first peak, broad off-specular diffuse scattering did not appear. Two sharp peaks at $\pm 0.0015\,\text{Å}^{-1}$ are the satellite peaks which are caused by double diffraction [7]. It is noted that, compared to X-ray scattering experiments, we can still observe the significant intensities where the incident angle to the sample or the grazing angle of the sample to the detector is beyond zero. At both limits only intensity dips centered at $\pm 0.001\,\text{Å}^{-1}$ in Fig. 7b and at $\pm 0.004\,\text{Å}^{-1}$ in Fig. 7c appear. This is because the neutron has much smaller absorption cross section than X-ray. It is clear that the profile of off-specular diffuse scattering outside the scan range of conventional X-ray off-specular reflection measurements gives us new information of multilayers. However, what information? From the contour map in Fig. 5, intensities of the diffuse scattering extend along the constant Q_z direction. Such a distribution of off-specular diffuse scattering indicates that the interfacial roughness has coherency from the bottom to the top layer [7]. Are the intensities also signals from the interfacial roughness in the multilayers? In order to answer the questions, we have measured the off-specular diffuse scattering of various Fe/Cr multilayers with different interfacial roughness.

Figs. 8–10 are the results of the Q_z and Q_r scans of sample 2–4 in several external magnetic fields. Intensities from different samples in these figures cannot be directly compared with each other because the dimensions of samples are not always the same. Sample 2 in Fig. 8 is a multilayer consisting of 51 Fe/Cr bilayers grown on MgO(1 0 0) substrate. The $\frac{1}{2}$ and the first peak appear more sharply than sample 1 in the Q_z scans. This indicates that sample 1 has more fluctuated lattice spacing of bilayers than sample 2. When the fluctuation is large, the multilayer is expected to have rather rough interfaces. If the roughness is not of magnetic origin, such roughness can be quantitatively measured using the conventional X-ray technique. In Fe/Cr multilayers the $\frac{1}{2}$ peak is pure magnetic Bragg peak. Thus, the neutron seems to be powerful tool for studying magnetic interfacial roughness, magnetic disorders at the interface, in the multilayers. However, in the small Q_r region we could not observe the obvious difference in the profile around the $\frac{1}{2}$ peaks between these two samples. This is due to the fact that TOPAN has much less experimental resolution than the X-ray spectrometers. Thus, we concentrate on the extra intensities which were observed in the transverse scan outside the scan limits of X-rays even though the diffuse scattering around the first peak shows the different aspects of the profile as seen in Fig. 7c and 8c.

On the contrary for the data in the small Q_r region, the clear difference of off-specular diffuse scattering appear outside the limits. In sample 2 large off-specular diffuse scattering was not observed around either the $\frac{1}{2}$ nor the first peak. Less

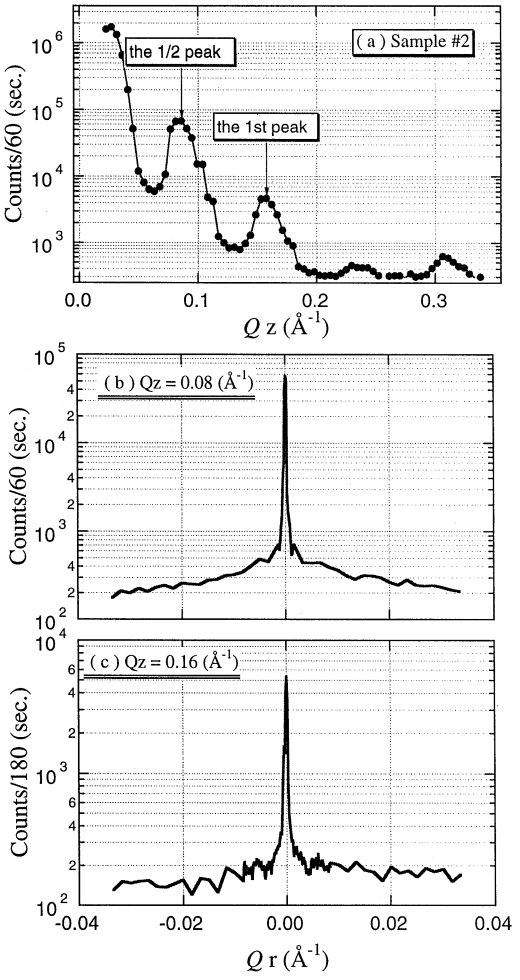

Fig. 8. The Q_z (a) and the Q_r scans, (b) and (c), for sample 2. This scan is exactly the same as in Fig. 7.

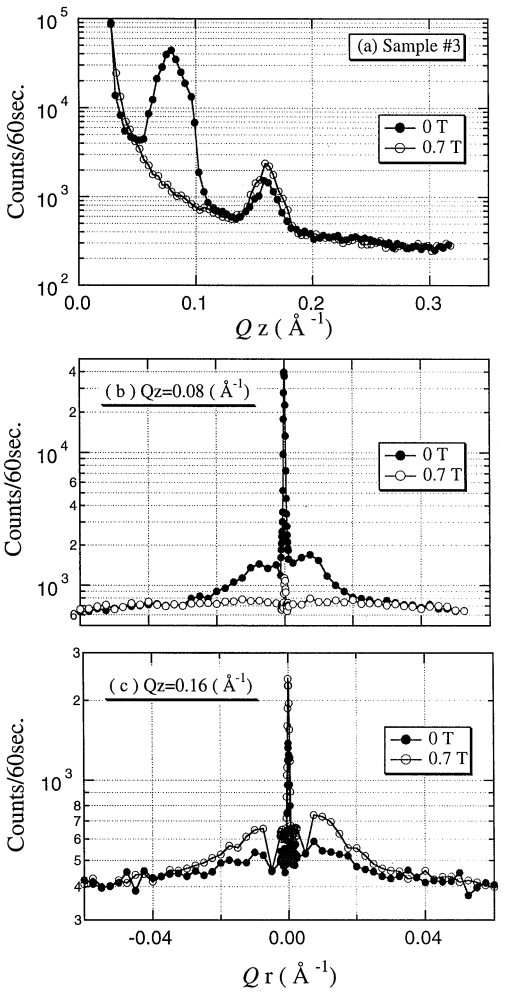

Fig. 9. The magnetic field dependence of the Q_z (a) and the Q_r scans, (b) and (c), for sample 3. Data in 0 T are plotterd by solid circles and that in the field of 0.7 T by open circles.

number of bilayers and a narrower Bragg peak in the Q_z scan suggest that sample 2 should have magnetically smoother interfaces than sample 1. At the first glance this leads to the conclusion that the rougher interface is accompanied by intense off-specular diffuse scattering. However, between these two samples there are the other factors besides the interfacial roughness which may cause the difference of off-specular diffuse scattering. These two samples have not been synthesized under exactly the same conditions. It is known that the different growth runs do not always give the same thickness of layers and quality of crystals in the superlattice, even though syntheses are done in the same manner. Figs. 10 and 11 show the data of samples 3 and 4 which have different substrates, Al_2O_3 (1 $\bar{1}$ 0 2) and MgO (1 0 0), and have been prepared simultaneously under the same growth run. The effect of the difference of substrates on MR ratio and magnetization has been carefully investigated and the clear substrate dependence was observed in Fe/Cr multilayers [6]. No abrupt or discontinuous change of the profiles was observed by applying external magnetic fields. Therefore, these figures show the data in antiferromagnetic

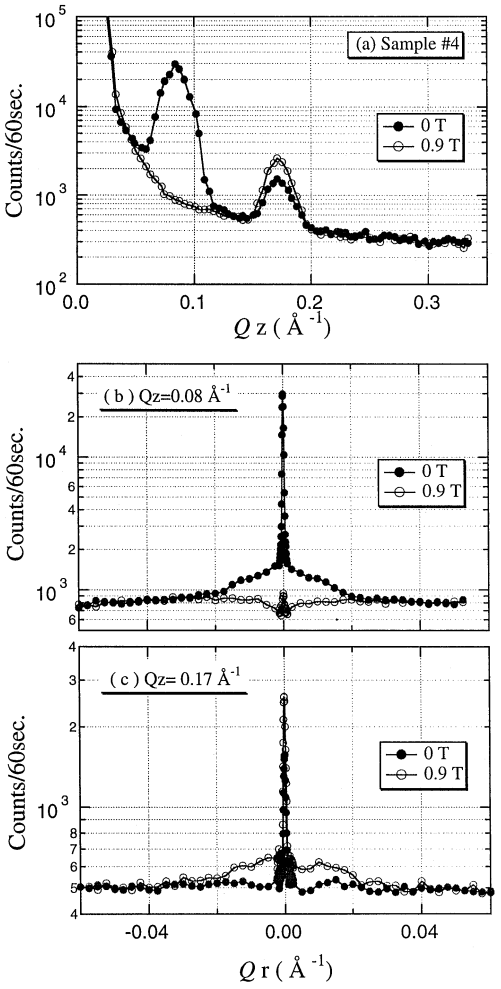

Fig. 10. The same measurements plotted in Fig. 9 for sample 4.

state of ferromagnetic Fe layers in the absence of external magnetic fields (solid circles) and in the forced ferromagnetic one induced by external magnetic fields (open circles). The intensities of the $\frac{1}{2}$ peaks decrease with increasing fields, and disappear in the ferromagnetic state. This is due to the fact that the antiferromagnetic alignment of the Fe layers goes to ferromagnetic one through the canting state. On the other hand, intensities of the first peak increases with increasing magnetic fields. The increase results from the ferromagnetic component of the Fe layers induced by the magnetic fields. It should be noted that there is no clear difference between two samples in the profile of Q_z scans.

In zero field, clear off-specular diffuse scattering appears around the 1/2 peak outside the limits (Fig. 9b and Fig. 10b), and a rather weak scattering was observed around the first peak (Fig. 9c) and Fig. 10c). When the magnetic fields were applied in the multilayers, the diffuse scattering around the $\frac{1}{2}$ peak was drastically suppressed in both samples, while the scattering is enhanced in the case of the first peak. The magnetic diffuse scattering around the $\frac{1}{2}$ peak disappears in the ferromagnetic state, however, a sharp peak remains at the Bragg peak position ($Q_r = 0$) even in this state. The sharp component originates from the intensity of the specular reflectivity curve. If the multilayers could have complete antiferromagnetic structures in zero external filed, the first peak would contain no magnetic information. The X-ray diffraction measurements of the Fe(2 0 0) and Cr(2 0 0) Bragg peaks of samples 3 and 4 revealed that a high-quality single crystal in the Fe/Cr multilayers was obtained and that the disorder on the atomic scale is negligible in the bulk Fe and Cr layers [6]. Therefore, the off-specular diffuse scattering observed around the 1st peak is considered to indicate the existence of atomic disorder at the interface. The enhancement of diffuse scattering around the first peak in the external magnetic fields suggests that the magnetic coherent disorder of ferromagnetic moments at the interface is induced by the magnetic fields. At the end of this section it is emphasized that the Q_r scan extends to the region outside the scan range of X-ray measurement and which makes the difference of samples evident.

4. Discussion

Various kind of physical surfaces can be described as a self-affine surface defined by Mandelbrot in terms of the fractional Brownian motion [8]. The reflection of X-ray and neutron from such surfaces is treated based on the self-affine surface model [9] and the theory has been extended to the multilayers with interfacial roughness [10–13]. For the multilayer system correlation between roughness at each interface from bottom to top layer has to be taken into consideration. The coherent interfacial roughness and roughness without correlation

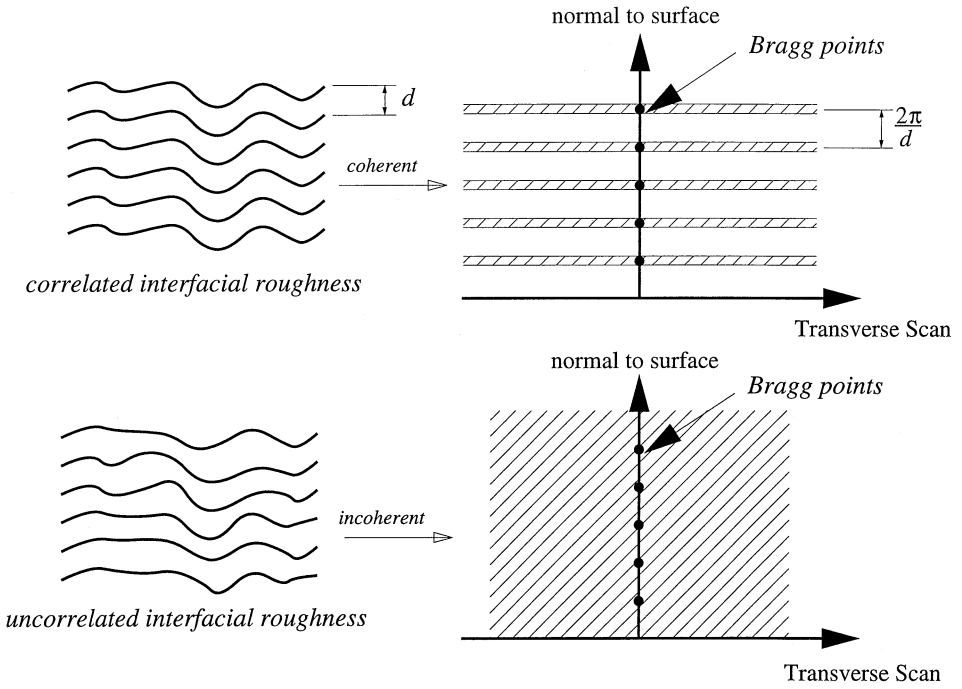

Fig. 11. Sketch of correlated and uncorrelated interfacial roughness and intensity distribution from the roughness in the reciprocal lattice.

between interfaces coexist in real multilayers. These two kind of roughnesses are highly correlated and the relation is not simple. Although there is presently no complete theory for interfacial roughness, it has been confirmed experimentally that intensities from the coherent roughness come together in the profile of the transverse scan at the Bragg points as schematically sketched in Fig. 11. On the other hand, X-ray and neutron reflected at the interfacial with incoherent roughness are diffusely scattered in all-the directions in the reciprocal space with no structures.

The diffuse scattering around the first peak without external magnetic fields can be attributed to the coherent atomic disorder at the interface. The atomic disorder at the interface may cause the magnetic disorder at the interface. Hence, we have speculated that magnetic diffuse scattering around the $\frac{1}{2}$ peak mainly originates from the magnetic disorder at the interfaces.

The off-specular magnetic diffuse scattering can be quantitatively analyzed by the same way as in the case of measurements of nonmagnetic multilayers using X-rays provided that the magnetic disorder at the interface is treated as a height distribution of homogeneous media with magnetic scattering length from the average smooth interface. This approximation ignores the fluctuation of direction of magnetic moments at the interfaces. It is not unique but one of the reasonable starting points of the quantitative analysis at the first stage. Here we have done the preliminary fitting by the following trial function,

$$I_{\mathrm{obs}}(Q_z, Q_{\mathrm{r}}) = 2\pi \frac{I_0 \exp(-Q_z^2\sigma^2)}{Q_z^2} \times \left[2\pi \frac{1}{\sqrt{2\pi}\sigma_{\mathrm{Bragg}}} \exp\left(-\frac{Q_{\mathrm{r}}^2}{2\sigma_{\mathrm{Bragg}}^2} \right) + \sum_{m=1}^{5} \frac{2\xi(Q_z^2\sigma^2)^m}{m(m!)} \frac{1}{1+(Q_{\mathrm{r}}\xi/m)^2} \right] + \text{background}, \quad (1)$$

where I_0 is the reflectivity of the multilayer with perfect surface and interfaces, σ the rms error of roughness, ξ the lateral correlation length, σ_{Bragg} is related to the experimental resolution. The function is the slightly modified one appearing in Ref. [7]. It assumes that the vertical displacement of interface from its average smooth interface has the exponential correlation function with respect to the lateral separation of two points on the interface. The first term is the specular reflection with experimental resolution and the second one expresses the off-specular diffuse scattering. In the actual measurements by using X-rays, there is unreachable regions in the reciprocal space where either they are shadowed by the sample or total reflection occurs. The original function of Eq. (1) can satisfactorily fit the experimental data of W/C multilayers within the limits. As mentioned in Section 3.2, the shadow effect is not so effective in the case of neutrons. The formulae describing the off-specular diffuse scattering seem to explicitly restrict the Q_r region concerning the shadow. The attenuation of reflected intensities should be accounted for the calculated profile as well as experimental resolution. Therefore, we neglected the other corrections except the resolution effect on the sharp specular component in the fitting. Fig. 12 shows two examples of the fitting where the experimental data of sample 3 in Fig. 9b and of 4 in Fig. 10b are plotted by open circles, and the results of the best fits are drawn by dashed-dotted lines. Whole profile of sample 3 cannot be simulated by using Eq. (1), while the fit for sample 4 is excellent, considering the simple model. The main difference of these two profiles is the peaks which appear at $Q_r = \pm 0.0075$ Å^{-1} in sample 3 but not in sample 4. At the Q_r, k_{i0} is parallel to the k_f (1 0 0) which satisfies the Bragg condition of the first peak, i.e. k_f (1 0 0) $- k_i$ (1 0 0) $= Q$ (1 0 0), or k_{f0} is parallel to the k_i (1 0 0). These peaks may be understood by the double diffraction in the multilayers like resonant peak appearing in the diffuse scattering [7]. In this case, however, this is a new feature because a detector is at the opposite side of reflection plane, and neutrons are detected after going through the samples. Anyway, the present preliminary fittings suggest that Eq. (1) is a good model function of magnetic interfacial roughness

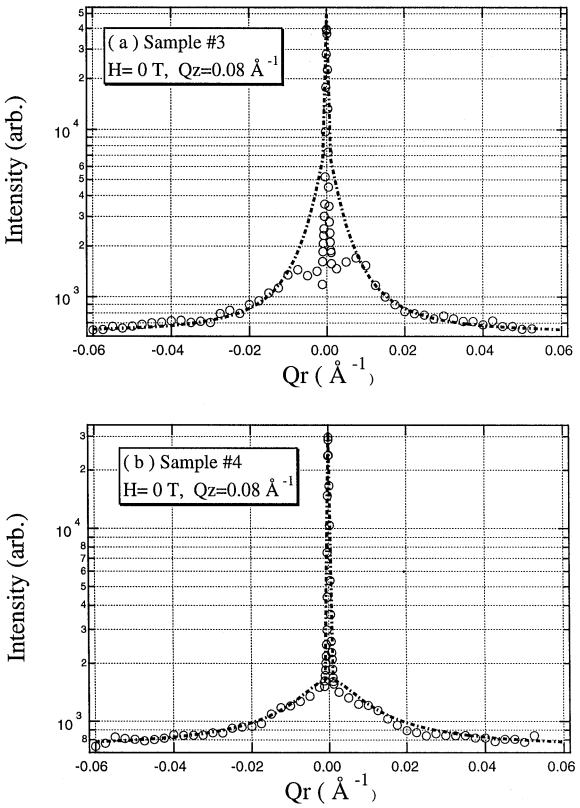

Fig. 12. Fits for the data of Q_r scans of sample 3 (a) and 4 (b) by a model function (see text).

in the Q_r region beyond the scan limits of X-ray measurements.

5. Conclusions

We performed the specular and off-specular diffuse scattering measurements of various Fe/Cr multilayers using both pulsed and monochromatic neutrons. In the multilayers it is found that the diffuse scattering around the Bragg peak from antiferromagnetic Fe/Cr bilayers is widely distributed along the direction normal to specular direction in the reciprocal lattice. The TOF spectrometer, TOP, could make useful contour maps of the intensity distribution in the wavelength of neutrons and the scattering angle plane. The profiles of the diffuse scattering have been measured as a function of the

Q_r on the conventional triple-axis spectrometer, TOPAN, in the various external magnetic fields. In the measurements the diffuse scattering was still detectable with a unique profile even under the condition that the incident angle exceeded zero degree due to the small absorption cross section. The extra diffuse intensity was associated with the antiferromagnetic Bragg peak, and the profile has been proved to vary with the external magnetic fields. The profiles were also very sensitive to the interfacial roughness. Therefore it is concluded that the diffuse scattering is related to magnetic disorder at the interface. In order to quantitatively analyze the diffuse intensities the more sophisticated fitting function is necessary. Finally, it should be emphasized that although the origin of extra off-specular diffuse scattering reported here has not been fully understood, it can be a very powerful tool to investigate the magnetic disorder at the interfaces in the magnetic multilayers.

Acknowledgements

We are indebted to Mr. H. Yasuda for the collaboration. We also thank Mr. M. Onodera and Mr. K. Nemoto for valuable technical assistance. This work was supported by a Grant-in-Aid for Scientific Research (A) (No. 03240102 and No. 05402011) and (C) (No. 06640463) from the Ministry of Education, Science, Sports and Culture.

References

[1] S. Ferrer, P. Fajardo, F. de Bergevin, J. Alvarez, X. Torrelles, H.A. van der Vegt, V.H. Etgens, Phys. Rev. Lett. 77 (1996) 747.
[2] Y. Yoneda, Phys. Rev. 131 (1963) 2010.
[3] M.N. Baibich, J.M. Broto, A. Fert, F. Nguyen Van Dau, F. Petroff, P. Eitenne, G. Creuzet, A. Friederich, J. Chazelas, Phys. Rev. Lett. 61 (1988) 2472.
[4] S.S.P. parkin, N. More, K.P. Roche, Phys. Rev. Lett. 64 (1990) 2304.
[5] A. Kamijo, J. Magn. Magn. Mater. 126 (1993) 59.
[6] A. Kamijo, S. Yamamoto, Mater. Sci. Eng. B 31 (1995) 169.
[7] D.E. Savage, J. Kleiner, N. Schimke, Y.-H. Phang, T. Jankowski, J. Jacobs, R. Kariotis, M.G. Lagally, J. Appl. Phys. 69 (1991) 1411.
[8] H.-O. Peitgen, D. Saupe, The Science of Fractal Images, Springer, New York, 1988.
[9] S.K. Sinha, E.B. Sirota, S. Garoff, H.B. Stanley, Phys. Rev. B 38 (1988) 2297.
[10] S.K. Sinha, Physica B 173 (1991) 25.
[11] J.B. Kortright, J. Appl. Phys. 70 (1991) 3620.
[12] D.E. Savage, Y.-H. Phang, J.J. Rownd, J.F. MaacKay, M.G. Lasgally, J. Appl. Phys. 74 (1993) 6158.
[13] D.G. Stearns, J. Appl. Phys 71 (1992) 4286.